Brain Structure and Function (2025) 230:110
https://doi.org/10.1007/s00429-025-02976-8

ORIGINAL ARTICLE

Individual uniqueness of connectivity gradients is driven by the complexity of the embedded networks and their dispersion

Yvonne Serhan[1,2] · Shaymaa Darawshy[1,2] · Wei Wei[3,4] · Daniel S. Margulies[3,4] · Karl-Heinz Nenning[5] · Smadar Ovadia-Caro[1,2]

Received: 4 December 2024 / Accepted: 18 June 2025

Abstract
Connectivity gradients are widely used to characterize meaningful principles of functional brain organization in health and disease. However, the degree of individual uniqueness and shared common principles is not yet fully understood. Here, we leveraged the Hangzhou test-retest dataset, comprising repeated resting-state fMRI scans over the span of 1 month, to investigate the balance between individual variation and shared patterns of brain organization. We quantified the short- and long-term stability for the first three connectivity gradients and used connectome fingerprinting to establish the associated individual identification rate. We found that all three connectivity gradients are highly correlated over both short and long time intervals, demonstrating connectome fingerprinting utility. Individual uniqueness was dictated by the complexity of the networks such that heteromodal networks had higher connectome fingerprinting rates than unimodal networks. Importantly, the dispersion of the gradient coefficients associated with canonical functional networks was correlated with identification rates, irrespective of the position along the gradients. Beyond individual uniqueness, between subject similarity was high along the first connectivity gradient, which captures the dissociation between unimodal and heteromodal cortices, and the second connectivity gradient, which differentiates sensory cortices. Our results support the usage of connectivity gradients for the purposes of both group comparisons and prediction of individual behaviours. Our work adds to existing knowledge on the shared versus unique organizational principles and offers insights into the importance of network dispersion to the individual uniqueness it carries.

Keywords Resting-state fMRI · Connectome fingerprinting · Identity analysis · Test-retest similarity · Dimensionality reduction

Introduction

Studying individual differences in brain-behavior associations based on features of brain organization relies on the premise that some organizational features are unique to individuals, stable over time and can be used as a proxy for individual behaviors, individual symptomatology and individual recovery (Damoiseaux et al. 2006; Finn et al. 2015; Fornito and Bullmore 2015; Gillebert and Mantini 2013; Ramduny and Kelly 2024; Shehzad et al. 2009). Understanding the intricate relationship between what is shared and what is unique to each individual constitutes a major challenge in neuroscience with both theoretical and practical implications.

The mapping of macroscale organization using intrinsic activity fluctuations measured with resting-state functional MRI (rs-fMRI) (Biswal et al. 1995) is offering a non-invasive

✉ Smadar Ovadia-Caro
sovadiaca@cog.haifa.ac.il

1 Department of Cognitive Sciences, School of Psychological Sciences, Faculty of Social Sciences, University of Haifa, Haifa, Israel

2 The Integrated Brain and Behavior Research Center (IBBRC), University of Haifa, Haifa, Israel

3 Centre National de la Recherche Scientifique, Université de Paris, INCC UMR 8002, Paris, France

4 The Oxford Centre for Integrative Neuroimaging, FMRIB, Nuffield Department of Clinical Neurosciences, University of Oxford, Oxford, United Kingdom, United Kingdom

5 Nathan S. Kline Institute for Psychiatric Research, Orangeburg, NY, USA

Published online: 03 July 2025

means for representing both features of segregation into distinct functional modules as well as their integration by hyperconnected networks (Bertolero et al. 2018; Bullmore and Sporns 2009; Cohen and D'Esposito 2016; van den Heuvel and Sporns 2011). Whereas a-priori parcellations are commonly used to overcome the high-dimensionality of rs-fMRI connectivity data (Gordon et al. 2016; Smith et al. 2009), more recently, data-driven, dimensionality reduction techniques are applied to represent a low-dimensional connectivity space, or connectivity axes, also termed *connectivity gradients* (Haak et al. 2018; Langs et al. 2014; Margulies et al. 2016).

The main strength of the approach is the continuity reflected in this representation along with the fundamental organizing principles it emphasizes. Brain regions are ranked along the axis of each connectivity gradient based on similarities in their whole-brain connectivity patterns (Huntenburg et al. 2018; Langs et al. 2014, 2016; Margulies et al. 2016), and different functional modules are therefore spread along each of the gradients in different locations yet in a clustered manner corresponding with well-known canonical functional networks (Hong et al. 2020; Huntenburg et al. 2018; Margulies et al. 2016). The fact that nodes are located along a continuum enables the adequate representation of both elements of segregation and integration. Whereas clustering of values reflects segregation and enhanced similarity of connectivity, integration is reflected in enhanced dispersion of values within a module, or an overlap of values between different modules. These changes in values correspond with 'contraction' or 'expansion' of the gradient as referred to in previous work (Knodt et al. 2023; Nenning et al. 2020; Ottoy et al. 2024). It is therefore that the *dispersion* of values is a mirror of both the modular topology and the connectedness of the nodes, or the network they are affiliated with.

From the representational perspective, the first connectivity gradient which is the one commonly used is reflecting a hierarchy such that primary sensory and unimodal networks are clustered at one end, whereas high-order, heteromodal networks and the default-mode network are at the other end (Margulies et al. 2016, 2022). This eminent orderly organizing principle (Mesulam 1998) emerging in a data-driven manner further supports the biological validity of the approach and provided the initial empirical support for its wide-usage. Beyond the first connectivity gradient, the second and third connectivity gradients usually emphasize different networks on their extremes (Bayrak et al. 2019; Margulies et al. 2022). Whereas the second connectivity gradient distinguishes the visual network from most other networks, the third connectivity gradient is demonstrating a different arrangement of networks such that areas of the frontoparietal and dorsal attention networks are situated at one end and areas of the default-mode network are situated on the other end. Different gradients therefore emphasize networks of different complexities on their extremes as well as different degrees of segregation or integration of these networks. Whereas along the first gradient, these two features correspond with one another as a continuum from unimodal to heteromodal, along the second gradient, a more subtle hierarchy within the visual network is captured, and the overall dispersion of this network is high. Gradients therefore contain both information on networks' complexity, or their hierarchical role (unimodal/heteromodal) in addition to their range of values, or dispersion, i.e., the degree to which they integrate via shared connectivity patterns.

Considering the advantages stated above, multiple studies in recent years have utilized connectivity gradients for both group comparisons and prediction of individual behaviour (Bayrak et al. 2019; Bernhardt et al. 2022; Bethlehem et al. 2020; Brown et al. 2022; Dong et al. 2023; Girn et al. 2022; Haak et al. 2018; Hong et al. 2019; Huntenburg et al. 2018; Knodt et al. 2023; Meng et al. 2021). However, the degree of similarity and the exploration of shared versus unique features captured along different gradients have not been directly investigated beyond the first connectivity gradient (Hong et al. 2020; Knodt et al. 2023). Since some studies are using multiple gradients and some even provide measures based on the combination of different gradients (Bethlehem et al. 2020), information on the shared and unique features of different gradients is essential to make informed analysis decisions fitted to the question at hand.

Here, we aimed at assessing the stability of connectivity gradients and their individual uniqueness using a subset of a freely-available test-retest data collected in Hangzhou University (Chen et al. 2015). Since individual test-retest reliability has been shown to decrease as intervals between the scans increase in multiple studies (Birn et al. 2013; Fiecas et al. 2013; Noble et al. 2017; O'Connor et al. 2017; Pannunzi et al. 2017; Shehzad et al. 2009), we chose to focus on both short-term interval (two scans separated by 3 days) and long-term interval (two scans separated by 1 month). Given the wealth of data supporting the functional significance of connectivity gradients in both group studies and as predictors of individual behaviors (Bayrak et al. 2019; Bernhardt et al. 2022; Bethlehem et al. 2020; Brown et al. 2022; Dong et al. 2023; Girn et al. 2022; Haak et al. 2018; Hong et al. 2019; Huntenburg et al. 2018; Knodt et al. 2023; Meng et al. 2021; Xia et al. 2022), as well as previous work addressing reliability of connectivity gradients (Hong et al. 2020; Knodt et al. 2023), we hypothesize that connectivity gradients will demonstrate high spatial similarity between different subjects, particularly for the first connectivity gradient. We additionally expect that connectivity gradients will be individually unique such that they will show high similarity

within subjects, sufficient for effective connectome fingerprinting (Ramduny and Kelly 2024; Finn et al. 2015). As for the factors influencing the effective fingerprinting, we hypothesize that the complexity of a network along the hierarchy and its dispersion will drive individual uniqueness. This hypothesis is supported by both empirical work showing high-order networks dominate individual uniqueness in parcellation-based studies (Finn et al. 2015; Blautzik et al. 2013; Marchitelli et al. 2017; Mejia et al. 2018; Noble et al. 2017, 2019; O'Connor et al. 2017; Somandepalli et al. 2015; Wisner et al. 2013; Zuo et al. 2014), as well as more theoretical accounts on the link between enhanced range and complex behaviors, where behavioral diversity is most likely to be expressed (Mesulam 1998, 2011; M.-M. Mesulam 1990).

Methods

Subjects' information

The current study is using a subset of the Hangzhou online available test-retest data (Chen et al. 2015). Thirty participants (age range 20–30 years, 15 females, mean age = 24, SD = 2.41) were recruited and repeatedly scanned over 1 month. Here, we used three consecutive rs-fMRI sessions from this dataset. The first two sessions were collected 3 days apart and the third session was collected 30 days after the first session (referred to here as days 1, 3, and 30). We used these three time points to investigate similarity over short and longer time intervals. Data collection was approved by the ethics committee of the Center for Cognition and Brain Disorders (CCBD) at the Hangzhou Normal University. Written informed consent was obtained from all participants.

MRI data acquisition

MRI imaging was performed using a GE MR750 3.0 Tesla scanner (GE Medical systems, Waukesha, WI) at CCBD at Hangzhou Normal University. Anatomical and functional MRI data were collected at each time point. A T1-weighted Fast Spoiled Gradient echo (FSPGR: TR = 8.06 ms, TE = 3.1 ms. TI = 450 ms, flip angle = 8°, field of view = 256 × 256, voxel size = 1 × 1 × 1 mm, 176 sagittal slices) was performed to acquire a high-resolution anatomical image. A 10-min T2-weighted echo-planar imaging (EPI: TR = 2000 ms, TE = 30ms, flip angle = 90°, field of view = 220 * 220 mm, matrix = 64 * 64, Voxel size = 3.4 * 3.4 * 3.4, 43 slices) sequence was performed to obtain functional images. The subjects had their eyes open, and a screen presented a black fixation point '+' in its center. The participants were instructed to relax and remain still with their eyes open, not to fall asleep, and not to think about anything in particular (Chen et al. 2015).

MRI data preprocessing

Imaging data were preprocessed using fMRIPrep 20.2.3 (Esteban et al. 2018, 2019). Anatomical preprocessing included: intensity non-uniformity (INU) correction, skull-stripping of the T1-weighted (T1w) reference image, and segmentation of cerebrospinal fluid (CSF), white matter (WM), and gray matter (GM). Reconstruction of brain surfaces was applied using recon-all from FreeSurfer 6.0.1 (Fischl 2012). T1w images from all three sessions were processed using FreeSurfer's mri_robust_template, as implemented in fMRIPrep (Esteban et al. 2019). A within-subject anatomical template was created by aligning all available T1w scans to the first session image, following FreeSurfer's standard cross-sectional processing stream. Spatial normalization to the MNI standard space (MNI152NLin2009cAsym) was performed using nonlinear registration with antsRegistration, using both brain-extracted anatomical and functional reference images. Functional preprocessing included the following steps for each of the three sessions per subject: motion correction, slice scan time correction, extraction of signals from the white matter and CSF masks, and extraction of a reference volume for functional to T1 registration by computing median over motion corrected file. Mean framewise displacement (FD) was computed for each subject across sessions to assess head motion. A threshold of 0.25 mm was applied. None of the subjects exceeded this threshold in any session, and thus all participants were retained for further analysis (see supplementary Fig S1). The denoising strategy was performed using load confound python package (https://github.com/SIMEXP/load_confounds) and included a minimal denoising strategy: regression of full motion parameters (24 parameters), white matter, CSF, and additional high pass filter to remove low-frequency drifts. The final file was transformed to a fsaverage5 surface template using mri_vol2surf (FreeSurfer) with 6 mm FWHM surface-based smoothing. Correlation matrix was then calculated for each MNI normalized dataset, resulting in 20,484 * 20,484 entries. This correlation matrix was fed to the dimensionality reduction algorithm.

Connectivity gradients analysis

Connectivity gradients represent axes of variance in the data by using techniques such as decomposition or embedding, which reduce the original dimensions while preserving most of the variability of the original data (Huntenburg et al. 2018). Each component therefore contains gradient

coefficient score coefficient values assigned to each vertex, indicating the similarity of global connectivity patterns among vertices. Gradients were computed using the BrainSpace Python toolbox (Vos de Wael et al. 2020). Specifically, for each scan, time series files were extracted for each vertex and correlation matrix was computed resulting in a 20,484 × 20,484 correlation matrix. An affinity matrix was derived using vertex-wise cosine similarity of the thresholded correlation matrix, where a default sparsity threshold of 0.9 was applied to retain the top 10% strongest connections vertex-wise. Principal component analysis (PCA) was then applied to the affinity matrix to extract gradients. Individual correlation matrices were fed to the dimensionality reduction algorithm, Principal Component Analysis (PCA) (Hong et al. 2020) resulting in 5 components/gradients for each subject and each scan. Gradient vectors were then aligned to a common template obtained on the HCP dense connectome matrix (Margulies et al. 2016; Van Essen et al. 2013) using the generalized Procrustes alignment approach (Vos de Wael et al. 2020). This choice of using only the first five components was based on previous work demonstrating they account for most of the variance in the original data, and work demonstrating that adding more components does not significantly enhance the explained variance for subsequent analysis (Bethlehem et al. 2020). Due to the predominant focus on the first gradient in previous research (Bernhardt et al. 2022) and the inherent interpretability challenges associated with multiple gradients, we have limited our analysis to the first three gradients. This decision is consistent with our previous work, which demonstrated that the first and third connectivity gradients serve as a biologically valid model (Bayrak et al. 2019), and with other studies that have identified behaviorally meaningful effects using these gradients (Hong et al. 2019) (see Supplementary Fig. S2 for explained variance as a function of gradient number). Importantly, considering additional dimensionality reduction techniques, such as diffusion embedding (Coifman et al. 2005), are commonly used in the field, the full analysis pipeline described below was additionally performed using diffusion embedding as implemented in BrainSpace (Vos de Wael et al. 2020). Briefly, default settings were used, including 0.9 sparsity threshold, and 10 iterations for Procrustes alignment (see Supplementary material M1 and Figs. S3–S7).

Similarity and individual identification analysis

To quantify how similar subjects are to themselves, Identification analysis, also known as connectome fingerprinting analysis was conducted similarly to previous work (Finn et al. 2015; Ramduny and Kelly 2024). First, to quantify stability over repeated tests, spatial similarity was calculated for each gradient using Pearson's correlation coefficient. Correlation was computed over vector pairs (day 1–day 3 and day 1–day 30) for all subjects yielding spatial similarity matrices for each session pairs (short and long-term) and for each connectivity gradient. Fingerprint analysis assigns an ID based on the highest matched correlation value (a 'winner take all approach'). Identification rates were therefore calculated as the proportion of correct classification of the same subjects as themselves over two sessions. To assess the statistical significance of identification rates, a non-parametric permutation test was then performed. In each iteration, subjects ID was permuted such that a 'correct' classification was assigned to a different subject to create a null distribution of ID accuracies. 1000 iterations were employed as previously done (Finn et al. 2015), p-value was computed based on the proportion of permutations in which the accuracy exceeded the observed (true) identification rate, Bonferroni correction (Bland and Altman 1995) was applied to adjust the p-values for multiple comparisons, and statistical significance was determined at an alpha level of 0.05.

To assess stability over repeated measurements within and between subjects, correlation was averaged for within-subjects values (along the diagonal) and between subjects values. A ratio of within/between subjects was calculated to reflect stability within individuals while taking into account correlation between subjects. We examined how this ratio varied across different gradients and whether it changed between sessions. A repeated-measures ANOVA was employed to assess the effect of the different gradients and different time intervals on this measure. The model included a subject-specific random effect to account for within-subject variability, with subjects as the error term. The full model examined the main effects of connectivity gradient and time, as well as their interaction. Additionally, post-hoc pairwise comparisons between the gradient levels were performed and the Bonferroni correction was used to adjust p-values for multiple comparisons, and statistical significance was determined at an alpha level of 0.05.

A-posteriori parcellation to networks

To address the relative contribution of different functional networks to the observed accuracy, a-posteriori parcellation (Thomas Yeo et al. 2011) to 6 canonical cortical networks was employed. The limbic network was omitted from our analysis due to low signal-to-noise ratio in these areas, which may inaccurately reflect connectivity among its regions through its wide range of values (Thomas Yeo et al. 2011). Gradient coefficient score values along each of the connectivity gradients were extracted for each network and ID analysis was then performed based on correlation obtained from each network using only the relevant vertices

in each parcel. To explore additional unimodal networks beyond sensorimotor and visual domains represented in Yeo's parcellation, the Cole-Anticevic Brain-wide Network Partition was additionally used in the same manner (Ji et al. 2018). This process resulted in the subdivision of the six networks into subsystems, yielding a total of 12 networks. This expansion encompasses the distinction between primary and secondary visual regions, as well as the inclusion of the auditory network. Ventral Multimodal (VMM) and Orbito-affective (ORA) parcels were excluded similarly to the approach we applied using Yeo's parcellation due to low signal-to-noise ratio and small network size for these two networks (Sanders et al. 2022). A total of 10 subnetworks was therefore used for further analyses. For each parcellation, comparisons across the three connectivity gradients were Bonferroni-corrected to control for multiple testing, resulting in adjusted p-values (p_{BON}). Statistical significance was determined at an alpha level of 0.05.

Network's complexity and dispersion

The networks were categorized into two groups: heteromodal and unimodal networks across both parcellations. To assess whether there were differences in accuracy rates between these groups, a Wilcoxon signed-rank test was performed in each parcellation separately. To determine whether changes in variance between sessions and gradients influenced the accuracy of the ID analysis, the variance in gradient coefficient score values was calculated for each network. Variance, in this context, serves as a measure of the dispersion of gradient coefficient score values within a specific network. Higher variance indicates a broader range, i.e., larger distribution of gradient coefficient score values and more integration along the continuum. Conversely, lower variance suggests a more uniform distribution, or a segregated connectivity pattern. A partial correlation analysis was performed to assess the relationship between variance and ID accuracy while controlling for the number of vertices in each network. Correlations were computed for each time interval (short and long) separately where percent accuracy was correlated with mean dispersion for each network calculated over the two relevant time points (short: day 1 and day 3; long: day 1 and day 30). Bonferroni-corrected p-values were calculated to account for four comparisons (2 time intervals × 2 parcellations), and statistical significance was determined at an alpha level of 0.05.

Variations in pre-processing

To examine how results were influenced by preprocessing decisions, the main analysis (pair-wise Pearson's correlation and identification accuracy) was performed for data preprocessed with additional removal of global signal regression as implemented in load confound python package (https://github.com/SIMEXP/load_confounds), and with varying thresholds of the affinity matrix (including 0, 50, 90 (used in the main analysis), 95, and 99%) using the BrainSpace Python toolbox (Vos de Wael et al. 2020) (see supplementary material M2. and Figs. S8, S9).

Combining multi-gradient information

To examine the potential utility of the usage of the joined information obtained over the first three gradients, gradient score values obtained via PCA decomposition with 90% threshold of affinity matrices were concatenated for each subject and each session. Pair-wise Pearson's correlation for short- and long-time intervals was calculated, and ID accuracy scores was calculated as done for the main analysis (see Supplementary Fig. S10).

All statistical analyses were performed using R Statistical Software (v4.5.0; R Core Team 2025).

Results

Gradient maps represent connectivity space on three axes based on shared connectivity patterns

To represent connectivity data on a lower-dimensional space, the first three connectivity gradients were extracted for each dataset individually. Following the application of PCA, each vertex receives a unitless gradient coefficient score value. Along each one of the gradients, vertices that share similar score values, share a similar global connectivity pattern. As a result, functional networks tend to cluster along specific gradients. The different gradients, however, implicate different networks on their extremes and therefore capture a different representation. Average group-maps over all subjects and all sessions (Fig. 1a) were calculated and an a-posteriori parcellation to six canonical networks (Thomas Yeo et al. 2011) was employed to visualize representations of the different networks and their location along the three gradients. Along the first gradient, heteromodal regions, such as the default mode network (DMN), exhibit high gradient coefficient score values and are clustered at one end of the gradient. In contrast, unimodal regions, including the sensorimotor network (SMN) and the visual network (VN), are positioned at the opposite end, reflecting a transition from unimodal to heteromodal networks. This hierarchical organization is consistent with the gradient structure previously reported (Margulies et al. 2016; Nenning et al. 2020), also for studies using different decomposition approaches (Bayrak et al. 2019; Hong et al. 2020). Different distinction

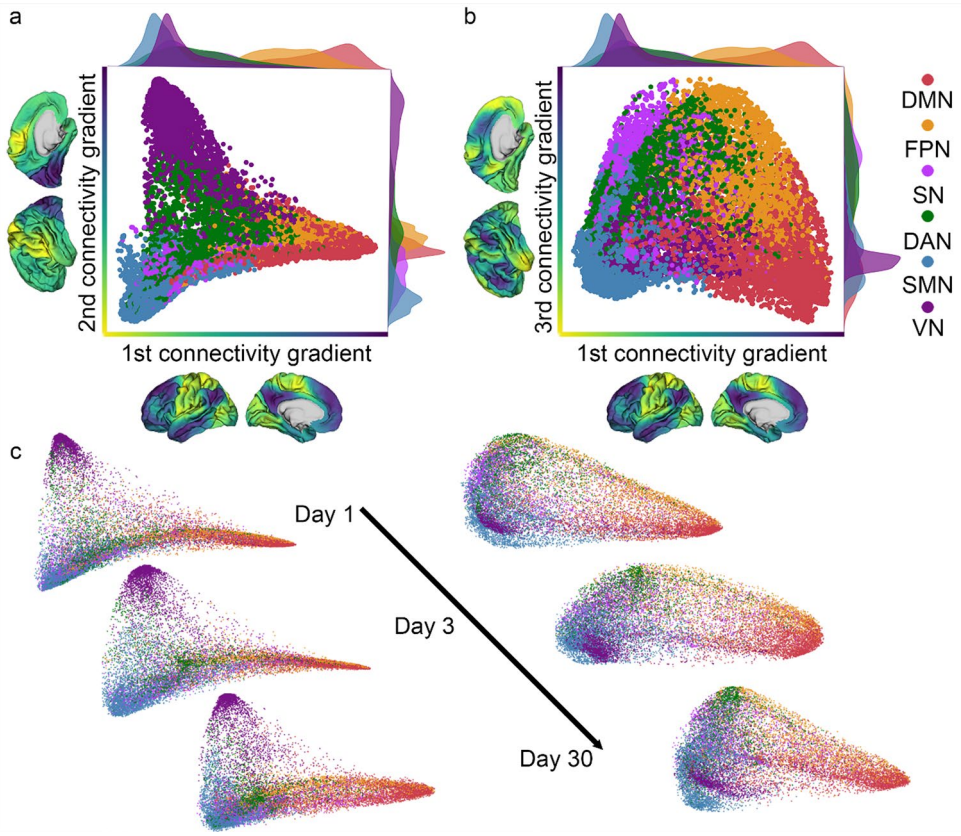

Fig. 1 Connectivity gradients represent a continuum based on similarity of functional connectivity patterns. **a** Average gradient coefficient score values for all subjects for each vertex, color coded according to Yeo's parcellation (Thomas Yeo et al. 2011). Along the first connectivity gradient (x-axis), a hierarchical gradient is captured such that default-mode network (DMN) is on the one end and sensorimotor network (SMN) and visual network (VN) are on the other end. Along the second connectivity gradient (y-axis) VN is distinguished from the SMN and most other networks. **b** Along the third connectivity gradient (y-axis), fronto-parietal network (FPN), dorsal attention network (DAN), and salience network (SN) are on the one end and DMN is on the other end. Different functional networks are represented in different locations along the different gradients, and each gradient captures a different representation. Along the different gradients, networks can change their dispersion of coefficient values. **c** Example data from an individual subject scanned over time. Connectivity space is represented along the first and second connectivity gradients (left), and along the first and third connectivity gradients (right). The general structure captured in the connectivity space is retained showcasing stability, yet slight changes are still evident over time

emerges along the second gradient, where the visual network (VN) is segregated from the sensorimotor network (SMN) and most other cortical regions. This differentiation highlights the dissociation of the visual system from most other functional networks. The third gradient captures a separation between different networks involved in higher-order cognitive functions. The frontoparietal network (FPN), dorsal attention network (DAN), and salience network (SN) are clustered together at one end, while the DMN is located at the opposite end of the gradient (Fig. 1b). The dispersion of values depicted in the density plots and the location of known networks changes in the different axes. The three connectivity gradients therefore capture different representations of functional networks and their respective segregation or integration along the continuum as reflected in the range of gradient coefficient score values. While this general layout is preserved in individual data demonstrating stability (Fig. 1c), some variation can still be observed over time thereby representing changes in the connectivity space within the same individual.

Connectivity gradients are stable within individuals over short and long-term periods

To quantify the stability of connectivity gradients over repeated measurements, Pearson's Correlation Coefficient was used to quantify spatial similarity. Correlation values were calculated between session pairs at day 1- day 3 and day 1- day 30, both within and between subjects, resulting in a separate correlation matrix for each gradient. The diagonal of the matrix shows correlation values for individual subjects across the different sessions (Fig. 2). Correlation values along the diagonal were generally higher than correlation values obtained for different subjects. All three

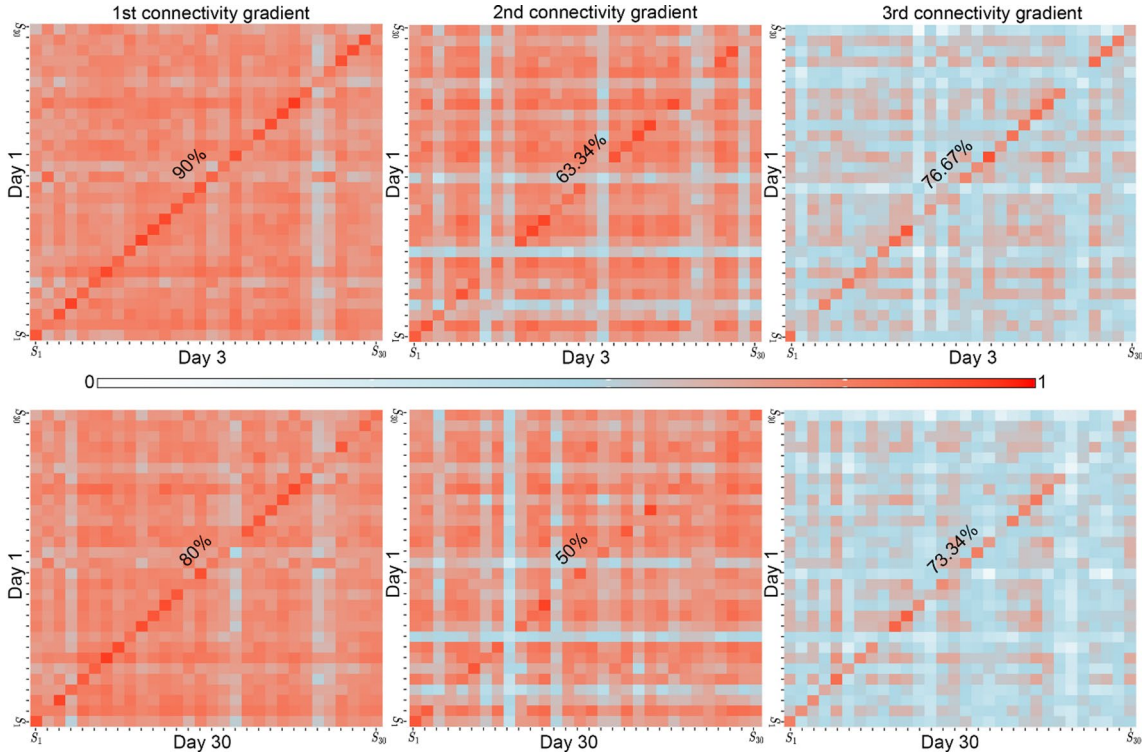

Fig. 2 Connectivity gradients are stable within individuals over short and long-term intervals. **a** Pearson's correlation coefficient values for connectivity gradients across subjects' data pairs. Along the diagonal, all three gradients show 'high' correlation values (mean r values > 0.79), indicating high stability within subjects. In the identification analysis, the first gradient demonstrates the highest accuracy rates with 90% for Day 1–Day 3, and 80% for Day 1–Day 30. The second gradient showed slightly lower accuracies: 63.34% for Day 1–Day 3, and 50% for Day 1–Day 30. The third gradient shows accuracies of 76.67% for Day 1–Day 3, and 73.34% for Day 1–Day 30. Connectivity gradients are therefore individually unique in both short and long-term intervals for all three connectivity gradients

connectivity gradients demonstrated 'high' correlation values (mean r values > 0.79, Fig. 3a) (Mukaka 2012) within individuals over both short and long time intervals. To examine if connectivity gradients can be effectively used for connectome fingerprinting, individual identification analysis (Finn et al. 2015) was performed. We found that for the first gradient accuracy rates were 90% for day 1–day 3, and 80% for day 1–day 30 cross prediction. For the second gradient, accuracy rates were 63.34% for day1–day 3, and 50% for day 1–day 30. For the third gradient, accuracy rates were 76.67% for day 1–day 3, and 73.34% for day 1–day 30. To assess the statistical significance of the identification accuracies, a nonparametric permutation test was performed. None of the permuted accuracies exceeded the observed accuracy rates, yielding p-values < 0.001 ($p_{BON} < 0.006$). Although accuracy rates were slightly lower for longer time intervals (30 days apart) compared to shorter ones (3 days apart), all three connectivity gradients reliably predicted individual brain organization, with the first gradient yielding the highest identification accuracy. A similar pattern of identification accuracies along the first three gradients was observed when using diffusion embedding for dimensionality reduction (Figs. S3, S4). Additionally, the significant identification rates over the first three gradients were invariant to changes in the pre-processing strategy including global signal regression, and varying thresholds of the connectivity matrices prior to decomposition, with the exception of 99% threshold of the affinity matrices demonstrating reduction in accuracy rates (see supplementary material M2 and Fig. S8–S9). Lastly, identification rates found over the first gradient were comparable to those observed when using all three gradients combined (see supplementary material M3 and Fig. S10) further supporting the contribution of the first gradient to the overall identification rate observed while taking combined gradients information into account.

The first and the second connectivity gradients are largely shared across different subjects

Beyond the high correlation values captured within the same subjects when re-scanned, considerable similarity exists between different subjects. Average correlation values between different subjects are in accordance with 'high' correlation for the first gradient and for the second gradient (mean r values > 0.71). Along the third gradient correlation drops to 'moderate' (Mukaka 2012) (mean r values = 0.5)

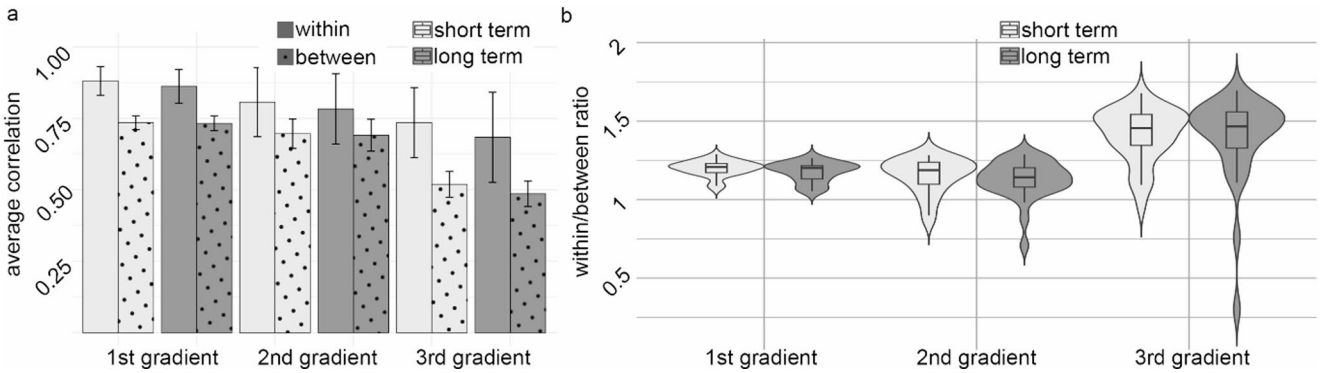

Fig. 3 Within/between correlation values for the three connectivity gradients over short and long intervals. **a** Average Pearson's correlation values for short-term (day 1–day 3) and long-term (day 1–30 days) sessions across the first, second, and third gradients, within (plain) and between (dotted) subjects. Bars represent mean values with standard error. Between subjects' correlation values are lower than within subjects' correlation values yet are high along the first and second connectivity gradients and moderate along the third connectivity gradient. Within subjects' correlation values are high along all three gradients and time intervals. **b** Within-to-between ratio distributions for short and long intervals across gradients. Violin plots display the distribution, box plots show the median and interquartile range, and whiskers represent variability. A value above 1 indicates higher correlation values for within-subject correlations compared to between-subject correlations. All three gradients show a mean ratio above 1. Significant differences were found between the first and third gradient and between the second and the third gradient

(Fig. 3a). To examine the relative contribution of within subject similarity taking between subjects' similarity into account, a ratio of within/between correlation was calculated (Fig. 3b). A significant main effect for 'gradient' was found in repeated measures ANOVA ($F(2,58) = 48.85$, $p_{BON} < 0.001$), indicating significant differences across gradients. No significant main effect was observed for 'time' ($F(1,29) = 1.144$, $p_{BON} = 0.294$), nor for interaction between 'gradient' and 'time' ($F(2,58) = 0.028$, $p_{BON} = 0.972$). Pairwise comparisons with Bonferroni correction (Bland and Altman 1995) revealed that Gradient G3 differed significantly from both G1 (mean difference = −0.219, SE = 0.037, $p_{BON} < 0.001$) and G2 (mean difference = −0.268, SE = 0.037, $p_{BON} < 0.001$). No significant difference was found between G1 and G2 ($p_{BON} = 0.570$). The same pattern of result was evident when using diffusion embedding for the decomposition (see Fig. S5).

Higher complexity of functional networks is associated with higher accuracy rates in identification analysis

To investigate the contribution of specific resting-state networks (RSNs) to the high identification accuracy rates observed at the whole gradient level, a-posteriori parcellation (Thomas Yeo et al. 2011) was applied to the three connectivity gradients (Fig. 4a) and identification analysis was repeated using gradient coefficient score values in each pre-defined network. Accuracy rates were compared for heteromodal networks, including the dorsal attention network (DAN), frontoparietal network (FPN), default mode network (DMN), and salience network (SN), with unimodal networks, including the somatomotor network (SMN) and visual network (VN). Heteromodal networks demonstrated significantly higher accuracy rates along the first ($p_{BON} = 0.02958$) and third ($p_{BON} < 0.001$) connectivity gradients. In contrast, along the second connectivity gradient, the visual network achieved moderate accuracies within the range of accuracies shown for other heteromodal networks and there is no significant difference between unimodal and heterometal networks ($p_{BON} = 1$). To complement our analysis with an additional, more detailed parcellation the same analysis was repeated using Cole parcellation (Fig. 4b). Similar trends were observed, where heteromodal networks, such as the Cingulo-Opercular Network (CON), Posterior Multimodal Network (PMM), and Language Network (LAN), demonstrated higher accuracy rates as compared with unimodal networks along the first ($p_{BON} < 0.001$) and third ($p_{BON} < 0.001$) connectivity gradients, and not along the second connectivity gradient ($p_{BON} = 0.4440$), where a reduction in accuracies over heteromodal networks was found. Interestingly, along the second connectivity gradient, the Visual 2 (VIS2) network achieved relatively high accuracies (76.67% for Day 1–Day 3, and 76.67% for Day 1–Day 30), while lower-order visual areas, Visual 1 (VIS1), showed slightly lower accuracies (70% for Day 1–Day 3, and 60% for Day 1–Day 30), and the overall accuracy over the second gradient seem to be driven by the visual network. These findings replicate and extend previous work (Finn et al. 2015; Blautzik et al. 2013; Marchitelli et al. 2017; Mejia et al. 2018; Noble et al. 2017, 2019; O'Connor et al. 2017; Somandepalli et al. 2015; Wisner et al. 2013; Zuo et al. 2014), supporting the role of high-order heteromodal networks in individual connectome fingerprinting. A similar

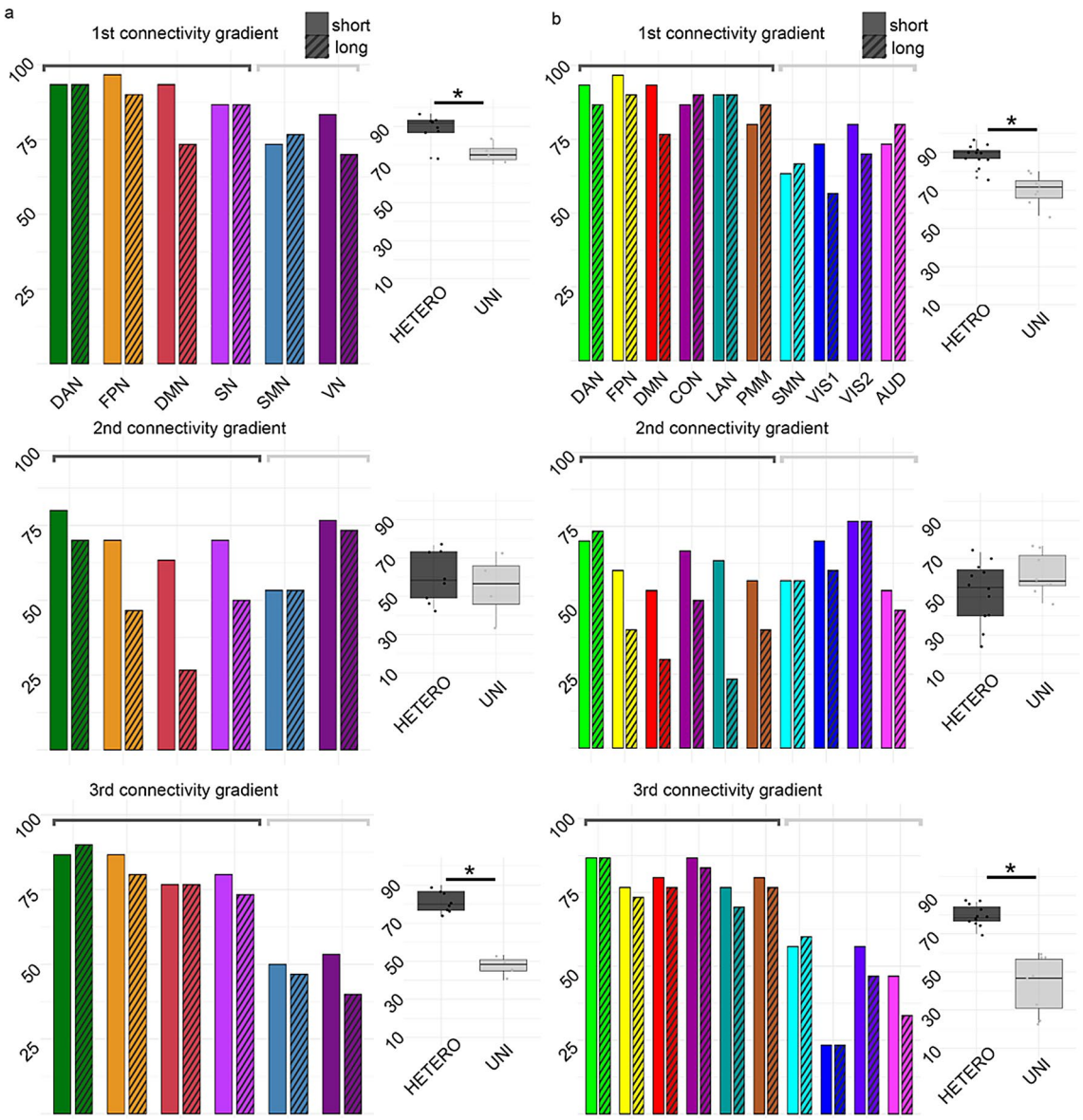

Fig. 4 Networks of higher complexity show higher accuracies in individual identification analysis. Accuracy rates for short-term (dashed bars) and long-term (plain bars) sessions across different brain networks for the first three connectivity gradients (left). Box plots comparing accuracy rates for heteromodal (HETERO) and unimodal networks (UNI) (right). **a** Accuracy rates for Yeo parcellation, including the Dorsal Attention Network (DAN), Frontoparietal Network (FPN), Default-mode Network (DMN), Salience Network (SN), Somatomotor Network (SMN), and Visual Network (VN). **b** Accuracy rates for Cole parcellation, incorporating the Cingulo-Opercular Network (CON), Language Network (LAN), Posterior Multimodal (PMM), Visual 2 (VIS2), Visual 1 (VIS1), and Auditory Network (AUD). Along the first and third gradients, networks of higher complexity show consistently higher rates of individual fingerprinting. Interestingly, along the second connectivity gradient, the visual network achieves high accuracy, but there is no significant difference between unimodal and heteromodal networks. A closer look shows that accuracy is slightly higher on VIS2, which represents higher-order visual areas, with less contribution from VIS1, representing low-order visual areas

pattern was found when using diffusion embedding for the decomposition thereby supporting generalizability to an additional, commonly used dimensionality reduction technique (Fig. S6).

Networks' dispersion is associated with higher accuracy rates in identification analysis

To investigate how dispersion is related to accuracy rates in the identification analysis, we correlated accuracy rates for short and long term in specific networks with their dispersion as measured by the variance of the average gradient

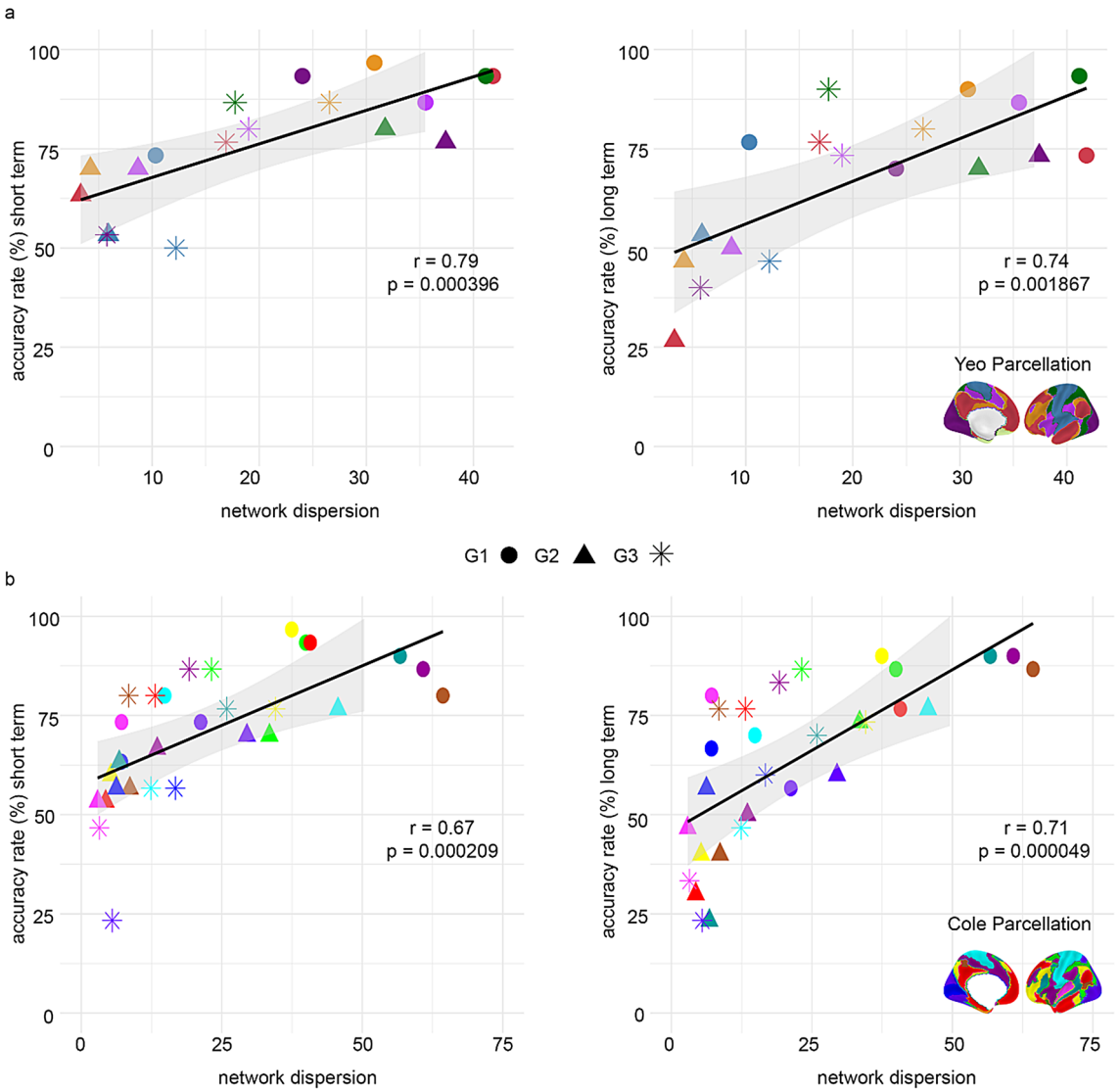

Fig. 5 Identity accuracies in networks positively correlate with their dispersion along the gradients and time intervals. Each point represents a network's mean dispersion along one of the first three connectivity gradients (G1–G3; denoted by marker shape) and its identification accuracy **a** Yeo parcellation; **b** Cole parcellation. Left panels show short-term accuracy (Day 1–Day 3) and corresponding average dispersion; right panels show long-term accuracy (Day 1–Day 30) and corresponding average dispersion. Each scatterplot presents a linear fit (black line) with 95% confidence interval (shaded area). Correlation values (Pearson's r) and Bonferroni-corrected p values are reported within each panel. In both parcellations, higher network dispersion is associated with higher accuracy rates, indicating that a broader range of connectivity leads to a more predictive network of individually unique organization. Brain maps illustrate corresponding networks for each parcellation

coefficient score values across first connectivity gradients and the corresponded gradient to the short term or long term. The results reveal a significant positive correlation between these two variables across both time intervals and parcellation schemes. Specifically, as network dispersion increases, accuracy increases, indicating that a broader range of connectivity contributes to more stable network gradient coefficient score values over time. This relationship was consistent across both the Yeo (short-term: r=0.79, $p_{BON} < 0.001$; long-term: r=0.74, p_{BON} = 0.001867) and Cole (short-term: r = 0.67, $p_{BON} < 0.001$; long-term: r=0.71, $p_{BON} < 0.001$) parcellations. A similar pattern was found when using diffusion embedding for the decomposition thereby supporting generalizability to an additional, commonly used dimensionality reduction technique (Figs. 5, S7).

Discussion

Here we aimed to assess the stability of connectivity gradients along the first three connectivity gradients and to determine if they can be used for effective connectome

fingerprinting over short and long-term time intervals. We additionally investigated how connectome fingerprint accuracies are influenced by the complexity of networks along the hierarchy and the dispersion of their gradient profiles.

We found that the first three connectivity gradients demonstrated high stability over time as measured by spatial correlation. Additionally, connectome fingerprinting based on correlation values demonstrated significantly high accuracy rates in all three connectivity gradients. While a modest reduction in correlation values and accuracy rates was observed after 1 month, effective fingerprinting was still retained, strengthening the robustness of gradient-based features for representing individual brain organization. This temporal stability suggests that connectivity gradients may capture core aspects of functional architecture that are resilient to transient fluctuations, potentially reflecting trait-like neural properties. In particular, the first and third gradients showed the highest identification accuracy over 30 days, highlighting their promise as candidates for imaging biomarkers. These findings align with previous work demonstrating that gradients are relatively robust to state-related changes (Cross et al. 2021) and maintain structural consistency even in pathological populations (Dong et al. 2023; Hong et al. 2019; Meng et al. 2021; Xia et al. 2022). Although our study did not include behavioral data, future research could investigate whether more stable traits such as personality are preferentially encoded by these gradients, thereby informing their utility in behavioral prediction and personalized neuroimaging.

When using a-posteriori defined parts of the gradients as a basis for connectome fingerprinting (Ji et al. 2018; Thomas Yeo et al. 2011), we found that the complexity of networks was associated with accuracy rates such that heteromodal networks showed higher accuracies as compared with unimodal networks. This result was observed along the first and the third gradient, but not the second gradient. A closer look into both the dispersion of gradient coefficients of the different networks and the specific emphasized representation along the second connectivity gradient provided an explanation for this result. The *gradient dispersion* measured by the variance of values in specific networks showed a significant positive correlation with the fingerprinting accuracy rates. This relationship was evident taking all gradients into account and using two different parcellations. In terms of representation, the second connectivity gradient demonstrates the dissociation between the visual and the somatosensory networks, while heteromodal networks are located at its center and the different heteromodal networks are therefore not well-distinguished from one another along this gradient. By using a more detailed parcellation, a difference emerged between visual networks and heteromodal networks such that fingerprinting accuracies were higher in visual areas, and more so in high-order visual areas. Taken together with the results of the first and the third gradient this suggests that network complexity and perhaps more importantly its dispersion along the gradients dictate fingerprinting performance.

Beyond the unique organization captured along the first three gradients, information contained in the gradients is also largely shared across participants. This is the case along the first and the second connectivity gradients showing high correlation values. In contrast, along the third connectivity gradient correlation values drop and are more moderate. When looking at the ratio of within to between subjects' similarity, we found that similarity within subjects was always higher than similarity between subjects setting average ratio values above one. Interestingly, along the third gradient, within subjects' similarity drops but to a lesser extent than between subjects' similarity, significantly increasing the ratio as compared with the first and the second gradients. This suggests that the third gradient becomes more variable across individuals.

Our results replicate previous work investigating test-retest reliability of the first connectivity gradient in different datasets (Hong et al. 2020; Knodt et al. 2023). Hong et al., have examined how variations in preprocessing influence reliability for the first 100 gradients (Hong et al. 2020), while more recently, Knodt et al., have directly compared reliability based on the first connectivity gradient to that of edgewise functional connectivity measures (Knodt et al. 2023). Both studies found good reliability for the first connectivity gradient (Hong et al. 2020; Knodt et al. 2023). Our study further extends previous work by investigating both stability in the first three gradients beyond the principle one and the associated connectome fingerprinting accuracy rates (Finn et al. 2015; Ramduny and Kelly 2024) spanned over short and long-term intervals. Connectome fingerprinting provides an intuitive and easily interpretable measure of connectome stability over time. By effectively demonstrating an individual can be identified in a group, numeric measures of agreement are complemented by a straightforward quantification of repeated measures stability (Ramduny and Kelly 2024). Our within subjects correlation values were slightly higher than those reported in Knodt et al., yet this can be explained by the a-priori spatial downsampling which was not implemented in our study yet is often implemented in gradients analysis (Vos de Wael et al. 2020). Retaining all vertices may thus improve reliability and associated accuracy rates for individual connectome fingerprinting.

The slight differences found here in terms of higher accuracy rates reported for the first and the third connectivity gradients can be linked with previous work emphasizing these two gradients in detecting the spread of individual

lesions within the functional connectome thereby suggesting stronger individual differences may be carried by these two gradients (Bayrak et al. 2019). Combined with the more variable ratio of within between reliability along the third gradient, this suggests combining the first and the third connectivity gradients may benefit analyses of individual behavioral predictions, however this is yet to be determined by future studies. Taken together, our findings strengthen the usage of the first three connectivity gradients as measures of individual brain organization stable over time. Overall, previous work establishing a link between connectivity gradients, individual behavior and symptomatology along mostly the first (Dong et al. 2023; Girn et al. 2022; Hong et al. 2019; Meng et al. 2021; Xia et al. 2022), but also secondary gradients (Bethlehem et al. 2020; Brown et al. 2022; Girn et al. 2022; Setton et al. 2022; Sydnor et al. 2021) further supports the functional relevance of the approach for prediction of individual cognitive behaviors.

Beyond demonstrating that connectivity gradients characterize individual features, information on the features that contribute to this uniqueness can be additionally drawn from our study. Different canonical networks are differently positioned along the continuum of the first three gradients. Additionally, the *dispersion of* network-specific gradient coefficients changes as well. Depending on the representation captured in a specific gradient, network dispersion varies, thereby enabling us to determine if it is associated with fingerprinting accuracy rates and how it relates to the complexity of the network. Previous work based on parcellation studies has established that specific networks are more predictive than others in terms of individual uniqueness. While there is some discrepancy, it is largely agreed that networks of higher complexity (i.e., heteromodal) and specifically frontal and default-mode networks are the most predictive of individual uniqueness (Blautzik et al. 2013; Marchitelli et al. 2017; Mejia et al. 2018; Noble et al. 2017, 2019; O'Connor et al. 2017; Somandepalli et al. 2015; Wisner et al. 2013; Zuo et al. 2014). Here, we replicate this result by showing that score values in heteromodal networks yield higher accuracy rates as compared with unimodal networks along the first and the third connectivity gradients, but not the second. This result highlights the importance of network complexity, or its hierarchical role. However, network positioning and its dispersion changes along different gradients. This creates a situation where a given network with a well-known hierarchical role can change its *range* in different gradients thereby reflecting a different element of its representation. Indeed, along the second gradient the dissociation between unimodal and heteromodal in terms of accuracy seems to fall out. However, a closer look is showing that dispersion of the visual networks is particularly high along this gradient, whereas heteromodal networks are located at its center, and are more segregated in terms of their dispersion. This suggests that the relationship between complexity and uniqueness is evident only when network dispersion is distributed enough to capture individual differences. Overall, we found that the dispersion of a given network is associated with accuracies irrespective of location along the different gradients. This result is in accordance with Knodt et al., where range has been shown to be associated with higher spatial correlation values (Knodt et al. 2023), as well as theoretical and evolutionary accounts of the 'untethering' of high-order cognitive areas from sensory ones (Buckner and Krienen 2013) and the distance between them as reflecting the flexible range that affords abstract cognitive functions (Mesulam 1998). Taking our results together with previous studies emphasizes that the dispersion, reflecting the degree of connectedness of a given network (van den Heuvel and Sporns 2013), is an important factor influencing uniqueness in addition to complexity. Larger range, or dispersion reflects a distributed and more reliable connectivity pattern. This is in accordance with previous work showing that variable connectivity across individuals is at the borders of core networks and is correlated with individual differences in behavior (Adelstein et al. 2011; Di Martino et al. 2009; Mennes et al. 2010; Nenning et al. 2023; Seitzman et al. 2019). Our result can explain some discrepancies in parcellation based studies showing visual networks are highly reliable within individuals (Blautzik et al. 2013; Chen et al. 2015; Noble et al. 2019; Shirer et al. 2015), and crucially stresses that the degree of network's integration is an important factor, even if not always independent, accompanying network complexity along the hierarchy in the prediction of individual brain signatures.

While the current study focused on characterizing the stability of connectivity gradients, rather than their predictive value for behavior, our findings nonetheless offer conceptual insights that may inform future research in this direction. The differential stability and identification accuracy observed across the first three gradients suggest that certain gradients, particularly the first and third, may offer greater potential for capturing stable, trait-like neural features relevant to individual differences. In contrast, the relatively high inter-subject similarity of the first and second gradients supports their utility for group-level comparisons or cross-sectional studies. Importantly, our finding that network dispersion correlates with individual identification rates points to a novel and potentially behaviorally relevant feature of the gradient framework. Dispersion may reflect the degree to which a network integrates across connectivity space, thereby capturing individual variability beyond what is offered by traditional edge-wise connectivity approaches. More generally, while component-based methods such as gradients offer a fine-grained representation of distinct

modes of variation within the connectome, their relative utility compared to edge-wise metrics in behavioral prediction remains an open and active area of research (e.g.,Knodt et al. 2023; Kong et al. 2023; Noble et al. 2019; Shevchenko et al. 2025). We suggest that future work systematically compare the predictive value of gradient-based and edge-based measures across behavioral domains and explore the role of dispersion as a potential biomarker of individual traits or cognitive function.

Investigating the spatial similarity between different subjects complements information on unique features of brain organization with those that are mutual. The high correlation values between subjects especially along the first and the second gradient suggests the representation captured in these gradients is mostly shared across people, promoting the adequacy of using the approach for group comparisons. This result is in line with studies demonstrating gradients are resilient to state-dependent changes following sleep deprivation (Cross et al. 2021) along with studies in monkeys demonstrating a similar organization (Buckner and Margulies 2019). Additionally, group studies that show differences in connectivity gradients, even in pathological versus healthy population (Dong et al. 2023; Hong et al. 2019; Meng et al. 2021; Xia et al. 2022) are expressing these differences in 'contraction' or 'expansion' of the gradients and not in dismantling of the order retained in the representation. Additional more methodological studies demonstrate the organization is preserved to a large extent even when different algorithms (Hong et al. 2020) or different thresholding strategies are used (Nenning et al. 2023). More generally, the representation captured along the first connectivity gradient is spanning two, largely antagonistic systems at its extremes. On the one end an intrinsic system dealing with our internal world and more abstract cognitive functions, and on the other end an extrinsic system dealing with our sensory world (Buckner et al. 2008; Buckner and Krienen 2013; Golland et al. 2007; Raichle and Snyder 2007; Smallwood et al. 2021). It is interesting to note that beyond the overt cognitive dissociation of these two systems, they tend to repeatedly emerge as separate entities in data driven analyses (Pines et al. 2022) thereby further supporting this representation as a fundamental organizing principle.

Our results should be interpreted considering several limitations. First, connectivity gradient analysis usually involves alignment of individual gradients to promote adequate comparison and mutual order of the gradients (Langs et al. 2015; Vos de Wael et al. 2020). As the approach is data-driven and the order of gradients is a byproduct of the explained variance, some variability exists in the order of gradients between individuals. Here, we did not examine how variable this factor is. Although alignment is a very common and acceptable practice in the field, future work should examine more systematically if individual order of gradients is in any way informative for individual fingerprinting. Second, our analysis was restricted to the first three connectivity gradients. This decision was driven by both the cumulative explained variance saturating quite rapidly after the first three gradients, in addition to the interpretability challenge associated with increased number of gradients, and the majority of brain-behavior studies using the approach focusing on the first, or the first several gradients (Bethlehem et al. 2020; Brown et al. 2022; Dong et al. 2023; Girn et al. 2022; Hong et al. 2019; Meng et al. 2021; Setton et al. 2022; Sydnor et al. 2021; Xia et al. 2022). However, recent work showing gradient-behavior prediction can improve using more than several gradients (Kong et al. 2023) suggest that more gradients may be relevant for predicting individual behavior. Lastly, we defined short- and long-term intervals as separated by 3 days and 30 days, respectively. This with the logic that individual signatures should be stable over long time periods, and the expected decay in stability over time. Future work should investigate the stability of gradients over longer time scales using repeated scanning spanned over longer time periods to support this claim (Laumann et al. 2015; Poldrack et al. 2015).

Conclusions

We have shown that the first three connectivity gradients are stable over time within individuals both on short and long-term intervals. Stability was accompanied by high accuracy rates demonstrating connectivity gradients can be effectively used for connectome fingerprinting purposes. When examining which features contribute to the individual uniqueness, we found that the dispersion of networks, along with their complexity in terms of hierarchical role are related to accuracy such that the higher the complexity is, and importantly the higher the dispersion is, the better accuracy rates are. This result was evident even when taking differences in network sizes into account, in two different parcellations, and importantly along the three different gradients where networks are located in different places on the continuum and can show differences in dispersion. Beyond the uniqueness, the first and the second connectivity gradients also showed high similarity between individuals demonstrating the organization captured along these two gradients is robust across participants and largely shared. Our study extends previous work on the shared versus unique organizational features and offers insights into the importance of network dispersion, i.e., the degree to which a given network shares connectivity with other networks, to the individual uniqueness it carries.

Data and code availability

The dataset used in this work are a subset of the freely available test-retest dataset from Hangzhou University (https://fcon_1000.projects.nitrc.org/indi/CoRR/html/hnu_1.html). The preprocessing and analyses code is available at https://github.com/SOC-PAB-Lab/Connectivity-Gradients-Stability.

Supplementary Information The online version contains supplementary material available at https://doi.org/10.1007/s00429-025-02976-8.

Acknowledgements The authors would like to kindly thank Dr. Yating Lv and Dr. Bella Vakulenko-Lagun for their advice on statistics and preprocessing. This work was supported by the Max-Planck Partner Group funding scheme; by the National Institute for Psychobiology in Israel Founded by the Charles E. Smith Family (Grant Number 25-20-21); and by the Alon Scholarship for the Integration of Outstanding Faculty (Israeli Council for Higher Education). Grants were obtained by Dr. Ovadia-Caro.

Author contributions Conceptualization, S.O.C., K.N and D.M.; Methodology, Y.S., S.D., W.W., and K.N.; Formal analysis, Y.S. and S.D.; Visualization, Y.S., W.W., and S.O.C; Writing—original draft, Y.S., K.N., and S.O.C.; writing—review and editing, Y.S., S.D., W.W., D.M., K.H.N., and S.O.C; Funding acquisition, S.O.C.; Supervision. S.O.C.

Funding Open access funding provided by University of Haifa.

Data availability The dataset used in this work are a subset of the freely available test-retest dataset from Hangzhou University (https://fcon_1000.projects.nitrc.org/indi/CoRR/html/hnu_1.html). The preprocessing and analyses code is available at https://github.com/SOC-PAB-Lab/Connectivity-Gradients-Stability.

Declarations

Competing interests The authors declare no competing interests.

References

Adelstein JS, Shehzad Z, Mennes M, DeYoung CG, Zuo X-N, Kelly C, Margulies DS, Bloomfield A, Gray JR, Castellanos FX, Milham MP (2011) Personality is reflected in the brain's intrinsic functional architecture. PLoS ONE 6(11):e27633. https://doi.org/10.1371/journal.pone.0027633

Bayrak Ş, Khalil AA, Villringer K, Fiebach JB, Villringer A, Margulies DS, Ovadia-Caro S (2019) The impact of ischemic stroke on connectivity gradients. NeuroImage Clin 24(April):101947. https://doi.org/10.1016/j.nicl.2019.101947

Bernhardt BC, Smallwood J, Keilholz S, Margulies DS (2022) Gradients in brain organization. NeuroImage 251:118987. https://doi.org/10.1016/j.neuroimage.2022.118987

Bertolero MA, Yeo BTT, Bassett DS, D'Esposito M (2018) A mechanistic model of connector hubs, modularity and cognition. Nat Hum Behav 2(10):765–777. https://doi.org/10.1038/s41562-018-0420-6

Bethlehem RAI, Paquola C, Seidlitz J, Ronan L, Bernhardt B, Consortium C-C, Tsvetanov KA (2020) Dispersion of functional gradients across the adult lifespan. *NeuroImage*, *222*, 117299. https://doi.org/10.1016/j.neuroimage.2020.117299

Birn RM, Molloy EK, Patriat R, Parker T, Meier TB, Kirk GR, Nair VA, Meyerand ME, Prabhakaran V (2013) The effect of scan length on the reliability of resting-state fMRI connectivity estimates. NeuroImage 83:550–558. https://doi.org/10.1016/j.neuroimage.2013.05.099

Biswal B, Zerrin Yetkin F, Haughton VM, Hyde JS (1995) Functional connectivity in the motor cortex of resting human brain using echo-planar mri. Magn Reson Med 34(4):537–541. https://doi.org/10.1002/mrm.1910340409

Bland JM, Altman DG (1995) Multiple significance tests: the bonferroni method. BMJ (Clin Res Ed) 310(6973):170. https://doi.org/10.1136/bmj.310.6973.170

Blautzik J, Keeser D, Berman A, Paolini M, Kirsch V, Mueller S, Coates U, Reiser M, Teipel SJ, Meindl T (2013) Long-term test-retest reliability of resting-state networks in healthy elderly subjects and with amnestic mild cognitive impairment patients. J Alzheimer's Disease: JAD 34(3):741–754. https://doi.org/10.3233/JAD-111970

Brown JA, Lee AJ, Pasquini L, Seeley WW (2022) A dynamic gradient architecture generates brain activity States. NeuroImage 261:119526. https://doi.org/10.1016/j.neuroimage.2022.119526

Buckner RL, Krienen FM (2013) The evolution of distributed association networks in the human brain. Trends Cogn Sci 17(12):648–665. https://doi.org/10.1016/j.tics.2013.09.017

Buckner RL, Margulies DS (2019) Macroscale cortical organization and a default-like apex transmodal network in the marmoset monkey. Nat Commun 10(1):1976. https://doi.org/10.1038/s41467-019-09812-8

Buckner RL, Andrews-Hanna JR, Schacter DL (2008) The brain's default network: anatomy, function, and relevance to disease. Ann N Y Acad Sci 1124:1–38. https://doi.org/10.1196/annals.1440.011

Bullmore E, Sporns O (2009) Complex brain networks: graph theoretical analysis of structural and functional systems. Nat Rev Neurosci 10(3):186–198. https://doi.org/10.1038/nrn2575

Chen B, Xu T, Zhou C, Wang L, Yang N, Wang Z, Dong HM, Yang Z, Zang YF, Zuo XN, Weng XC (2015) Individual variability and test-retest reliability revealed by ten repeated resting-state brain scans over one month. PLoS ONE 10(12):1–21. https://doi.org/10.1371/journal.pone.0144963

Chen G, Taylor PA, Haller SP, Kircanski K, Stoddard J, Pine DS, Leibenluft E, Brotman MA, Cox RW (2018) Intraclass correlation: improved modeling approaches and applications for neuroimaging. Hum Brain Mapp 39(3):1187–1206. https://doi.org/10.1002/hbm.23909

Cohen JR, D'Esposito M (2016) The segregation and integration of distinct brain networks and their relationship to cognition. J Neuroscience: Official J Soc Neurosci 36(48):12083–12094. https://doi.org/10.1523/JNEUROSCI.2965-15.2016

Coifman RR, Lafon S, Lee AB, Maggioni M, Nadler B, Warner F, Zucker SW (2005) Geometric diffusions as a tool for harmonic analysis and structure definition of data: diffusion maps. Proc Natl Acad Sci 102(21):7426–7431. https://doi.org/10.1073/pnas.0500334102

Cross N, Paquola C, Pomares FB, Perrault AA, Jegou A, Nguyen A, Aydin U, Bernhardt BC, Grova C, Dang-Vu TT (2021) Cortical gradients of functional connectivity are robust to state-dependent changes following sleep deprivation. NeuroImage 226:117547. https://doi.org/10.1016/j.neuroimage.2020.117547

Damoiseaux JS, Rombouts SaRB, Barkhof F, Scheltens P, Stam CJ, Smith SM, Beckmann CF (2006) Consistent resting-state networks across healthy subjects. Proc Natl Acad Sci USA 103(37):13848–13853. https://doi.org/10.1073/pnas.0601417103

Vos de Wael R, Benkarim O, Paquola C, Lariviere S, Royer J, Tavakol S, Xu T, Hong S-J, Langs G, Valk S, Misic B, Milham M, Margulies D, Smallwood J, Bernhardt BC (2020) BrainSpace: A toolbox for the analysis of macroscale gradients in neuroimaging and connectomics datasets. Commun Biology 3:103. https://doi.org/10.1038/s42003-020-0794-7

Di Martino A, Shehzad Z, Kelly C, Roy AK, Gee DG, Uddin LQ, Gotimer K, Klein DF, Castellanos FX, Milham MP (2009) Relationship between Cingulo-Insular functional connectivity and autistic traits in neurotypical adults. Am J Psychiatry 166(8):891–899. https://doi.org/10.1176/appi.ajp.2009.08121894

Dong D, Wang Y, Zhou F, Chang X, Qiu J, Feng T, He Q, Lei X, Chen H (2023) Functional connectome hierarchy in schizotypy and its associations with expression of Schizophrenia-related genes. Schizophr Bull. https://doi.org/10.1093/schbul/sbad179

Esteban O, Blair R, Markiewicz CJ, Berleant SL, Moodie C, Ma F (2018) FMRIPrep [Software]. Zenodo. https://doi.org/10.5281/zenodo.852659

Esteban O, Markiewicz CJ, Blair RW, Moodie CA, Isik AI, Erramuzpe A, Kent JD, Goncalves M, DuPre E, Snyder M, Oya H, Ghosh SS, Wright J, Durnez J, Poldrack RA, Gorgolewski KJ (2019) FMRIPrep: a robust preprocessing pipeline for functional MRI. Nat Methods 16(1):111–116. https://doi.org/10.1038/s41592-018-0235-4

Fiecas M, Ombao H, van Lunen D, Baumgartner R, Coimbra A, Feng D (2013) Quantifying temporal correlations: a test-retest evaluation of functional connectivity in resting-state fMRI. NeuroImage 65:231–241. https://doi.org/10.1016/j.neuroimage.2012.09.052

Finn ES, Shen X, Scheinost D, Rosenberg MD, Huang J, Chun MM, Papademetris X, Constable RT (2015) Functional connectome fingerprinting: identifying individuals using patterns of brain connectivity. Nat Neurosci 18(11):1664–1671. https://doi.org/10.1038/nn.4135

Fischl B (2012) FreeSurfer. NeuroImage 62(2):774–781. https://doi.org/10.1016/j.neuroimage.2012.01.021

Fornito A, Bullmore ET (2015) Connectomics: a new paradigm for understanding brain disease. Eur Neuropsychopharmacol 25(5):733–748. https://doi.org/10.1016/j.euroneuro.2014.02.011

Gillebert CR, Mantini D (2013) Functional connectivity in the normal and injured brain. Neuroscientist: Rev J Bringing Neurobiol Neurol Psychiatry 19(5):509–522. https://doi.org/10.1177/1073858412463168

Girn M, Roseman L, Bernhardt B, Smallwood J, Carhart-Harris R, Nathan Spreng R (2022) Serotonergic psychedelic drugs LSD and psilocybin reduce the hierarchical differentiation of unimodal and transmodal cortex. NeuroImage 256:119220. https://doi.org/10.1016/j.neuroimage.2022.119220

Golland Y, Bentin S, Gelbard H, Benjamini Y, Heller R, Nir Y, Hasson U, Malach R (2007) Extrinsic and intrinsic systems in the posterior cortex of the human brain revealed during natural sensory stimulation. Cereb Cortex (New York, NY: 1991) 17(4):766–777. https://doi.org/10.1093/cercor/bhk030

Gordon EM, Laumann TO, Adeyemo B, Huckins JF, Kelley WM, Petersen SE (2016) Generation and evaluation of a cortical area parcellation from resting-state correlations. Cerebral Cortex (New York, NY.: 1991) 26(1):288–303. https://doi.org/10.1093/cercor/bhu239

Gorgolewski K, Burns CD, Madison C, Clark D, Halchenko YO, Waskom ML, Ghosh SS (2011) Nipype: a flexible, lightweight and extensible neuroimaging data processing framework in Python. Front Neuroinf. https://doi.org/10.3389/fninf.2011.00013

Gorgolewski KJ, Esteban O, Markiewicz CJ, Ziegler E, Ellis DG, Notter MP, Jarecka D et al (2018) "Nipype." Software. https://doi.org/10.5281/zenodo.596855

Haak KV, Marquand AF, Beckmann CF (2018) Connectopic mapping with resting-state fMRI. NeuroImage 170:83–94. https://doi.org/10.1016/j.neuroimage.2017.06.075

Hong SJ, de Wael RV, Bethlehem RAI, Lariviere S, Paquola C, Valk SL, Milham MP, Di Martino A, Margulies DS, Smallwood J, Bernhardt BC (2019) Atypical functional connectome hierarchy in autism. Nat Commun 10(1):1–13. https://doi.org/10.1038/s41467-019-08944-1

Hong SJ, Xu T, Nikolaidis A, Smallwood J, Margulies DS, Bernhardt B, Vogelstein J, Milham MP (2020) Toward a connectivity gradient-based framework for reproducible biomarker discovery. NeuroImage. https://doi.org/10.1016/j.neuroimage.2020.117322

Huntenburg JM, Bazin PL, Margulies DS (2018) Large-scale gradients in human cortical organization. Trends Cogn Sci 22(1):21–31. https://doi.org/10.1016/j.tics.2017.11.002

Ji JL, Spronk M, Kulkarni K, Repov G, Anticevic A, Cole MW (2018) Mapping the human brain's cortical-subcortical functional network organization. Neuroimage.https://doi.org/10.1016/j.neuroimage.2018.10.006

Knodt AR, Elliott ML, Whitman ET, Winn A, Addae A, Ireland D, Poulton R, Ramrakha S, Caspi A, Moffitt TE, Hariri AR (2023) Test–retest reliability and predictive utility of a macroscale principal functional connectivity gradient. Hum Brain Mapp 44(18):6399–6417. https://doi.org/10.1002/hbm.26517

Kong R, Tan YR, Wulan N, Ooi LQR, Farahibozorg S-R, Harrison S, Bijsterbosch JD, Bernhardt BC, Eickhoff S, Yeo T, B. T (2023) Comparison between gradients and parcellations for functional connectivity prediction of behavior. NeuroImage 273:120044. https://doi.org/10.1016/j.neuroimage.2023.120044

Langs G, Sweet A, Lashkari D, Tie Y, Rigolo L, Golby AJ, Golland P (2014) Decoupling function and anatomy in atlases of functional connectivity patterns: language mapping in tumor patients. NeuroImage 103:462–475. https://doi.org/10.1016/j.neuroimage.2014.08.029

Langs G, Golland P, Ghosh SS (2015) LNCS 9350—Predicting activation across individuals with Resting-State functional connectivity baseNeuroimageabel fusion. https://doi.org/10.1007/978-3-319-24571-3_38

Langs G, Wang D, Golland P, Mueller S, Pan R, Sabuncu MR, Sun W, Li K, Liu H (2016) Identifying shared brain networks in individuals by decoupling functional and anatomical variability. Cereb Cortex 26(10):4004–4014. https://doi.org/10.1093/cercor/bhv189

Laumann TO, Gordon EM, Adeyemo B, Snyder AZ, Joo SJ, Chen M-Y, Gilmore AW, McDermott KB, Nelson SM, Dosenbach NUF, Schlaggar BL, Mumford JA, Poldrack RA, Petersen SE (2015) Functional system and areal organization of a highly sampled individual human brain. Neuron 87(3):657–670. https://doi.org/10.1016/j.neuron.2015.06.037

Marchitelli R, Collignon O, Jovicich J (2017) Test-Retest reproducibility of the intrinsic default mode network: influence of functional magnetic resonance imaging Slice-Order acquisition and Head-Motion correction methods. Brain Connect 7(2):69–83. https://doi.org/10.1089/brain.2016.0450

Margulies DS, Ghosh SS, Goulas A, Falkiewicz M, Huntenburg JM, Langs G, Bezgin G, Eickhoff SB, Castellanos FX, Petrides M, Jefferies E, Smallwood J (2016) Situating the default-mode network along a principal gradient of macroscale cortical organization. Proc Natl Acad Sci USA 113(44):12574–12579. https://doi.org/10.1073/pnas.1608282113

Margulies DS, Ovadia-Caro S, Saadon-Grosman N, Bernhardt B, Jefferies B, Smallwood J (2022) Cortical Gradients and Their Role in Cognition. In S. Della Sala (Ed.), *Encyclopedia of Behavioral Neuroscience, 2nd edition (Second Edition)* (pp. 242–250). Elsevier. https://doi.org/10.1016/B978-0-12-819641-0.00010-4

Mejia AF, Nebel MB, Barber AD, Choe AS, Pekar JJ, Caffo BS, Lindquist MA (2018) Improved Estimation of subject-level functional connectivity using full and partial correlation with empirical Bayes shrinkage. NeuroImage 172:478–491. https://doi.org/10.1016/j.neuroimage.2018.01.029

Meng Y, Yang S, Chen H, Li J, Xu Q, Zhang Q, Lu G, Zhang Z, Liao W (2021) Systematically disrupted functional gradient of the cortical connectome in generalized epilepsy: initial discovery and independent sample replication. NeuroImage 230:117831. https://doi.org/10.1016/j.neuroimage.2021.117831

Mennes M, Kelly C, Zuo X-N, Di Martino A, Biswal BB, Castellanos FX, Milham MP (2010) Inter-individual differences in resting-state functional connectivity predict task-induced BOLD activity. NeuroImage 50(4):1690–1701. https://doi.org/10.1016/j.neuroimage.2010.01.002

Mesulam M-M (1990) Large-scale neurocognitive networks and distributed processing for attention, language, and memory. Ann Neurol 28(5):597–613. https://doi.org/10.1002/ana.410280502

Mesulam MM (1998) From sensation to cognition. Brain 121(6):1013–1052. https://doi.org/10.1093/brain/121.6.1013

Mesulam M (2011) The evolving landscape of human cortical connectivity: facts and inferences ☆. https://doi.org/10.1016/j.neuroimage.2011.12.033

Mukaka M (2012) A guide to appropriate use of correlation coefficient in medical research. Malawi Med Journal: J Med Association Malawi 24(3):69–71

Nenning K-H, Xu T, Schwartz E, Arroyo J, Woehrer A, Franco AR, Vogelstein JT, Margulies DS, Liu H, Smallwood J, Milham MP, Langs G (2020) Joint embedding: A scalable alignment to compare individuals in a connectivity space. NeuroImage 222:117232. https://doi.org/10.1016/j.neuroimage.2020.117232

Nenning K-H, Xu T, Franco AR, Swallow KM, Tambini A, Margulies DS, Smallwood J, Colcombe SJ, Milham MP (2023) Omnipresence of the sensorimotor-association axis topography in the human connectome. NeuroImage 272:120059. https://doi.org/10.1016/j.neuroimage.2023.120059

Noble S, Spann MN, Tokoglu F, Shen X, Constable RT, Scheinost D (2017) Influences on the Test-Retest Reliability of Functional Connectivity MRI and its Relationship with Behavioral Utility. *Cerebral Cortex (New York, N.Y.: 1991)*, *27*(11), 5415–5429. https://doi.org/10.1093/cercor/bhx230

Noble S, Scheinost D, Todd Constable R (2019) A decade of test-retest reliability of functional connectivity: A systematic review and meta-analysis. https://doi.org/10.1016/j.neuroimage.2019.116157

O'Connor D, Potler NV, Kovacs M, Xu T, Ai L, Pellman J, Vanderwal T, Parra LC, Cohen S, Ghosh S, Escalera J, Grant-Villegas N, Osman Y, Bui A, Craddock RC, Milham MP (2017) The healthy brain network serial scanning initiative: A resource for evaluating inter-individual differences and their reliabilities across scan conditions and sessions. GigaScience 6(2):1–14. https://doi.org/10.1093/gigascience/giw011

Ottoy J, Kang MS, Tan JXM, Boone L, de Wael V, Park R, Bezgin B, Lussier G, Pascoal FZ, Rahmouni TA, Stevenson N, Fernandez Arias J, Therriault J, Hong J, Stefanovic S-J, McLaurin B, Soucy J, Gauthier J-P, Bernhardt S, Goubran BC, M (2024) Tau follows principal axes of functional and structural brain organization in alzheimer's disease. Nat Commun 15(1):5031. https://doi.org/10.1038/s41467-024-49300-2

Pannunzi M, Hindriks R, Bettinardi RG, Wenger E, Lisofsky N, Martensson J, Butler O, Filevich E, Becker M, Lochstet M, Kühn S, Deco G (2017) Resting-state fMRI correlations: from link-wise unreliability to whole brain stability. NeuroImage 157:250–262. https://doi.org/10.1016/j.neuroimage.2017.06.006

Pines AR, Larsen B, Cui Z, Sydnor VJ, Bertolero MA, Adebimpe A, Alexander-Bloch AF, Davatzikos C, Fair DA, Gur RC, Gur RE, Li H, Milham MP, Moore TM, Murtha K, Parkes L, Thompson-Schill SL, Shanmugan S, Shinohara RT, Satterthwaite TD (2022) Dissociable multi-scale patterns of development in personalized brain networks. Nat Commun 13(1):2647. https://doi.org/10.1038/s41467-022-30244-4

Poldrack RA, Laumann TO, Koyejo O, Gregory B, Hover A, Chen M-Y, Gorgolewski KJ, Luci J, Joo SJ, Boyd RL, Hunicke-Smith S, Simpson ZB, Caven T, Sochat V, Shine JM, Gordon E, Snyder AZ, Adeyemo B, Petersen SE, Mumford JA (2015) Long-term neural and physiological phenotyping of a single human. Nat Commun 6:8885. https://doi.org/10.1038/ncomms9885

R Core Team (2025) R: a language and environment for statistical computing. R Foundation for Statistical Computing, Vienna. https://www.R-project.org/

Raichle ME, Snyder AZ (2007) A default mode of brain function: a brief history of an evolving idea. NeuroImage 37(4):1083–1090; discussion 1097–1099. https://doi.org/10.1016/j.neuroimage.2007.02.041

Ramduny J, Kelly C (2024) Connectome-based fingerprinting: reproducibility, precision, and behavioral prediction. Neuropsychopharmacology. https://doi.org/10.1038/s41386-024-01962-8

Sanders AFP, Baum GL, Harms MP, Kandala S, Bookheimer SY, Dapretto M, Somerville LH, Thomas KM, Van Essen DC, Yacoub E, Barch DM (2022) Developmental trajectories of cortical thickness by functional brain network: the roles of pubertal timing and socioeconomic status. Dev Cogn Neurosci 57:101145. https://doi.org/10.1016/j.dcn.2022.101145

Seitzman BA, Gratton C, Laumann TO, Gordon EM, Adeyemo B, Dworetsky A, Kraus BT, Gilmore AW, Berg JJ, Ortega M, Nguyen A, Greene DJ, McDermott KB, Nelson SM, Lessov-Schlaggar CN, Schlaggar BL, Dosenbach NUF, Petersen SE (2019) Trait-like variants in human functional brain networks. Proc Natl Acad Sci USA 116(45):22851–22861. https://doi.org/10.1073/pnas.1902932116

Setton R, Mwilambwe-Tshilobo L, Girn M, Lockrow AW, Baracchini G, Hughes C, Lowe AJ, Cassidy BN, Li J, Luh W-M, Bzdok D, Leahy RM, Ge T, Margulies DS, Misic B, Bernhardt BC, Stevens WD, De Brigard F, Kundu P, Spreng RN (2022) Age differences in the functional architecture of the human brain. Cereb Cortex (New York, NY: 1991) 33(1):114–134. https://doi.org/10.1093/cercor/bhac056

Shehzad Z, Kelly AMC, Reiss PT, Gee DG, Gotimer K, Uddin LQ, Lee SH, Margulies DS, Roy AK, Biswal BB, Petkova E, Castellanos FX, Milham MP (2009) The resting brain: unconstrained yet reliable. Cereb Cortex (New York, NY: 1991) 19(10):2209–2229. https://doi.org/10.1093/cercor/bhn256

Shevchenko V, Benn RA, Scholz R, Wei W, Pallavicini C, Klatzmann U, Alberti F, Satterthwaite TD, Wassermann D, Bazin P-L, Margulies DS (2025) A comparative machine learning study of schizophrenia biomarkers derived from functional connectivity. Sci Rep 15(1):2849. https://doi.org/10.1038/s41598-024-84152-2

Shirer WR, Jiang H, Price CM, Ng B, Greicius MD (2015) Optimization of rs-fMRI pre-processing for enhanced signal-noise separation, test-retest reliability, and group discrimination. NeuroImage 117:67–79. https://doi.org/10.1016/j.neuroimage.2015.05.015

Shrout PE, Fleiss JL (1979) Intraclass correlations: uses in assessing rater reliability. Psychol Bull 86(2):420–428

Smallwood J, Bernhardt BC, Leech R, Bzdok D, Jefferies E, Margulies DS (2021) The default mode network in cognition: a topographical perspective. Nat Rev Neurosci 22(8):503–513. https://doi.org/10.1038/s41583-021-00474-4

Smith SM, Fox PT, Miller KL, Glahn DC, Fox PM, Mackay CE, Filippini N, Watkins KE, Toro R, Laird AR, Beckmann CF (2009) Correspondence of the brain's functional architecture during activation and rest. Proc Natl Acad Sci 106(31):13040–13045. https://doi.org/10.1073/pnas.0905267106

Somandepalli K, Kelly C, Reiss PT, Zuo X-N, Craddock RC, Yan C-G, Petkova E, Castellanos FX, Milham MP, Di Martino A (2015) Short-term test-retest reliability of resting state fMRI metrics in children with and without attention-deficit/hyperactivity disorder. Dev Cogn Neurosci 15:83–93. https://doi.org/10.1016/j.dcn.2015.08.003

Sydnor VJ, Larsen B, Bassett DS, Alexander-Bloch A, Fair DA, Liston C, Mackey AP, Milham MP, Pines A, Roalf DR, Seidlitz J, Xu T, Raznahan A, Satterthwaite TD (2021) Neurodevelopment of the association cortices: patterns, mechanisms, and implications for psychopathology. Neuron 109(18):2820–2846. https://doi.org/10.1016/j.neuron.2021.06.016

Thomas Yeo BT, Krienen FM, Sepulcre J, Sabuncu MR, Lashkari D, Hollinshead M, Roffman JL, Smoller JW, Zöllei L, Polimeni JR, Fisch B, Liu H, Buckner RL (2011) The organization of the human cerebral cortex estimated by intrinsic functional connectivity. J Neurophysiol 106(3):1125–1165. https://doi.org/10.1152/jn.00338.2011

van den Heuvel MP, Sporns O (2011) Rich-club organization of the human connectome. J Neuroscience: Official J Soc Neurosci 31(44):15775–15786. https://doi.org/10.1523/JNEUROSCI.3539-11.2011

Van Essen, D. C., Smith, S. M., Barch, D. M., Behrens, T. E., Yacoub, E., Ugurbil, K., & Wu-Minn HCP Consortium. (2013). The WU-Minn human connectome project: an overview. Neuroimage 80:62–79.

van den Heuvel MP, Sporns O (2013) Network hubs in the human brain. Trends Cogn Sci 17(12):683–696. https://doi.org/10.1016/j.tics.2013.09.012

Wisner KM, Atluri G, Lim KO, Macdonald AW (2013) Neurometrics of intrinsic connectivity networks at rest using fMRI: retest reliability and cross-validation using a meta-level method. NeuroImage 76:236–251. https://doi.org/10.1016/j.neuroimage.2013.02.066

Xia M, Liu J, Mechelli A, Sun X, Ma Q, Wang X, Wei D, Chen Y, Liu B, Huang C-C, Zheng Y, Wu Y, Chen T, Cheng Y, Xu X, Gong Q, Si T, Qiu S, Lin C-P, He Y (2022) Connectome gradient dysfunction in major depression and its association with gene expression profiles and treatment outcomes. Mol Psychiatry 27(3):1384–1393. https://doi.org/10.1038/s41380-022-01519-5

Zuo XN, Anderson JS, Bellec P, Birn RM, Biswal BB, Blautzik J, Breitner JCS, Buckner RL, Calhoun VD, Castellanos FX, Chen A, Chen B, Chen J, Chen X, Colcombe SJ, Courtney W, Craddock RC, Di Martino A, Dong HM, Milham MP (2014) An open science resource for Establishing reliability and reproducibility in functional connectomics. Sci Data 1:1–13. https://doi.org/10.1038/sdata.2014.49